

DeepTag: inferring diagnoses from clinical notes in under-resourced medical domain

Allen Nie^{1,+}, Ashley Zehnder^{1,+}, Rodney L. Page², Arturo Lopez Pineda¹, Manuel A. Rivas¹, Carlos D. Bustamante^{1,3}, and James Zou^{1,3,*}

¹Department of Biomedical Data Science, Stanford University, Stanford, CA 94305, USA

²Department of Clinical Sciences, Colorado State University, Fort Collins, CO 80523, USA

³Chan-Zuckerberg Biohub, San Francisco, CA 94158, USA

*jamesz@stanford.edu

+these authors contributed equally to this work

ABSTRACT

Large scale veterinary clinical records can become a powerful resource for patient care and research. However clinicians lack the time and resource to annotate patient records with standard medical diagnostic codes and most veterinary visits are captured in free text notes. The lack of standard coding makes it challenging to use the clinical data to improve patient care. It is also a major impediment to cross-species translational research, which relies on the ability to accurately identify patient cohorts with specific diagnostic criteria in humans and animals. In order to reduce the coding burden for veterinary clinical practice and aid translational research, we have developed a deep learning algorithm, DeepTag, which automatically infers diagnostic codes from veterinary free text notes. DeepTag is trained on a newly curated dataset of 112,558 veterinary notes manually annotated by experts. DeepTag extends multi-task LSTM with an improved hierarchical objective that captures the semantic structures between diseases. To foster human-machine collaboration, DeepTag also learns to abstain in examples when it is uncertain and defers them to human experts, resulting in improved performance. DeepTag accurately infers disease codes from free text even in challenging cross-hospital settings where the text comes from different clinical settings than the ones used for training. It enables automated disease annotation across a broad range of clinical diagnoses with minimal pre-processing. The technical framework in this work can be applied in other medical domains that currently lack medical coding resources.

Introduction

While a robust medical coding infrastructure exists in the US healthcare system for human medical records, this is not the case in veterinary medicine, which is under-resourced in the sense that it lacks coding infrastructure and standardized nomenclatures across medical institutions. Most veterinary clinical notes are not coded with standard SNOMED-CT diagnosis¹. This hampers efforts at clinical research and public health monitoring. Due to the relative ease of obtaining large volumes of free-text veterinary clinical records for research (compared to similar volumes of human medical data) and the importance of turning these volumes of text into structured data to advance clinical research, we investigated effective methods for building automatic coding systems for the veterinary records.

It is becoming increasingly accepted that spontaneous diseases in animals have important translational impact on the study of human disease for a variety of disciplines². Beyond the study of zoonotic diseases, which represent 60-70% of all emerging

diseases^a, non-infectious diseases, like cancer, have become increasingly studied in companion animals as a way to mitigate some of the problems with rodent models of disease³. Additionally, spontaneous models of disease in companion animals are being used in drug development pipelines as these models more closely resemble the “real world” clinical settings of diseases than genetically altered mouse models⁴⁻⁷. However, when it comes to identifying clinical cohorts of veterinary patients on a large scale for clinical research, there are several problems. One of the first is that veterinary clinical visits rarely have diagnostic codes applied to them, either by clinicians or medical coders. There is no substantial third party payer system and no HealthIT act that applies to veterinary medicine, so there are few incentives for clinicians or hospitals to annotate their records for diseases to be able to identify patients by diagnosis. Billing codes are largely institution-specific and rarely applicable across institutions, unless hospitals are under the same management struc-

^a<https://wwwnc.cdc.gov/eid/page/zoonoses-2018>

ture and records system. Some large corporate practice groups have their own internal clinical coding structures, but that data is rarely made available for outside researchers. A small number (< 5) academic veterinary centers (of a total of 30 veterinary schools in the US)^b employ dedicated medical coding staff that apply disease codes to clinical records so these records can be identified for clinical faculty for research purposes. How best to utilize this rare, well-annotated, veterinary clinical data for the development of tools that can help organize the remaining segments of the veterinary medical domain is an open area of research.

In this paper, we develop DeepTag, a system to automatically code veterinary clinical notes. DeepTag takes free-form veterinary note as input and infers clinical diagnosis from the note. The inferred diagnosis is in the form of SNOMED-CT codes. We trained DeepTag on a large set of 112,558 veterinary notes, and each note is expert labeled with a set of SNOMED-CT codes. DeepTag is a bidirectional long-short term memory network (BLSTM) augmented with a hierarchical training objective that captures similarities between the diagnosis codes. We evaluated DeepTag's performance on challenging cross-hospital coding tasks.

Related work Natural language processing (NLP) techniques have improved from leveraging discrete patterns such as n-grams⁸ to continuous learning algorithms like Long-short-term Memory Networks (LSTMs)⁹. This strategy has proven to be extremely successful when a sizable amount of data can be acquired. Combined with advances in optimization and classification algorithms, the field has developed algorithms that match or exceed human performance in traditionally difficult tasks in multiple domains¹⁰.

Analyzing free text such as diagnostic reports and clinical notes has been a central focus of clinical natural language processing¹¹. Most of the previous research has focused on the human healthcare systems. Examples include using NLP tools to improve pneumonia screening in the emergency department, assisting in adenoma detection, assisting and simplifying hospital processes by identifying billing codes from clinical notes¹². Pivovarov et al. have conducted experiments to discover phenotypes and diseases using an unsupervised method on a broad set of heterogeneous data¹³.

In the domain of veterinary medicine, millions

of clinical summaries are stored as electronic health records (EHR) in various hospitals and clinics. Unlike human discharge summaries that have been assigned with billing codes (ICD-9/ICD-10 codes), veterinary summaries exist primarily as free text. This makes it challenging to perform systematic analysis such as disease prevalence studies, analysis of adverse drug effects, therapeutic efficacy or outcome analysis. Veterinary domain is very favorable for an NLP system that can convert large amount of free-text notes into structured information. Such a system would benefit the veterinary community in a substantial way and can be deployed in multiple clinical settings. Veterinary medicine is a domain where clinical NLP tools can have a substantial impact in practice and be integrated into daily use.

Identifying a set of conditions/diseases from clinical notes has been actively studied^{12,14}. Currently, the task of transforming free text into structured information primarily relies on two approaches: named entity recognition (NER) and automated coding. DeepTag is designed to perform automated coding rather than NER. NER requires annotation on the word level, where each word is associated with one of a few types. In the ShARe task¹⁵, the importance is placed on identifying disease span and then normalizing into standard terminology in SNOMED-CT or UMLS (Unified Medical Language System). In other works, the focus has been on tagging each word with a specific type: adverse drug effect, severity, drug name, etc¹⁶. Annotating on word level is expensive, and most corpora contain only a couple of hundreds or thousands of clinical notes. Even though early shared task in this domain has proven to be successful^{17,18}, it is still difficult to curate a large dataset in this manner.

Automated coding on the other hand takes the entire free text as input, and infers a set of labels that are used to code the entire work. Most discharge summaries in human hospitals have billing codes assigned. Baumel et al. proposed a text processing model for automated coding that processes each sentence first and then processes the encoded hidden states for the entire document¹⁹. This multi-level approach is especially suitable for longer texts, and the method was applied to the MIMIC data, where each document is on average five times longer than the veterinary notes from CSU. Rajkomar et al. used deep learning methods to process the entire EHR and make clinical predictions for a wide range of problems including automated coding²⁰. In their work,

^b<http://aavmc.org/>

they compared three deep learning models: LSTM, time-aware feedforward neural network (TANN), and boosted time-based decision stumps. In this work, we use a new hierarchical training objective which is designed to capture the similarities among the SNOMED-CT codes. This hierarchical objective is complementary to these previous approaches in the sense that the hierarchical objective can be used on top of any architecture. Our cross-hospital evaluations also extend what is typically done in literature. Even though Rajkomar et al. had data from two hospitals, they did not investigate the performance of the model when trained on one hospital but evaluated on the other. In our work, due to the lack of coded clinical notes in the veterinary community beyond a few academic hospitals, it is especially salient for us to evaluate the model’s ability to generalize across hospitals.

Our work is also related to the work of Kavuluru et al., who experimented with different training strategies and compared which strategy is the best for automated coding²¹, and Subotin et al., who improved upon direct label probability estimation and used a conditional probability estimator to fine-tune the label probability²². Perotte et al. also investigated possible methods to leverage the hierarchical structure of disease labels by using an SVM algorithm on each level of the ICD-9 hierarchy tree²³.

Cross-hospital generalization is a significant challenge in the veterinary coding setting. Most veterinary clinics currently do not apply diagnosis codes to their notes¹. Therefore our training data can only come from a handful of university-based regional referral centers that manually code their free text notes. The task is to train a model on such data and deploy for thousands of private hospitals and clinics. University-based centers and private hospitals and clinics have substantial variation in the writing style, the patient population, and the distribution of diseases (Figure 1b). For example, the training dataset we have used in this work comes from a university-based hospital with a high-volume referral oncology service, but typical local hospitals might face more dermatologic or gastrointestinal cases.

Results

DeepTag takes clinician’s notes as input and predicts a set of SNOMED-CT disease codes. SNOMED-CT is a comprehensive and precise clinical health terminology managed by the International Health Terminology Standards Development Organization.

DeepTag is a bi-directional long short-term memory (LSTM) neural network with a new hierarchical learning objective designed to capture similarities between the SNOMED-CT codes.

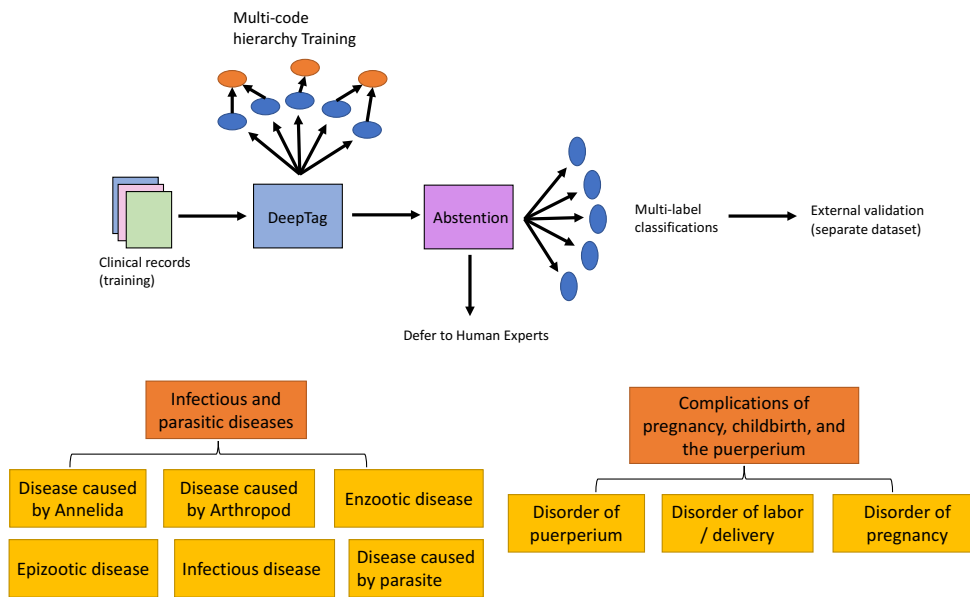
DeepTag is trained on 112,558 annotated veterinary notes from the Colorado State University of Veterinary Medicine and Biomedical Sciences (CSU) for research purposes. Each of these notes is a free text description of a patient visit, and is manually labeled with at least one, but on average eight, SNOMED-CT codes by experts. When the coder-applied disease codes that are mapped up to the children of parent note *Disease (disorder)* (ConceptID: 64572001), there are 41 SNOMED-CT top-level disease codes present in the CSU dataset. In addition, we map every non-disease related code to an extra spurious code. In total, DeepTag learns to tag a clinical note with a subset of 42 codes.

We evaluate DeepTag on two different datasets. One consists of 5,628 randomly sampled non-overlapping documents from the same CSU dataset that the system is trained on. The other dataset contains 586 documents and are collected from a private practice (PP) located in northern California. Each of these documents is also manually annotated with the appropriate SNOMED-CT codes by human experts. We refer to this dataset as the PP dataset. We regard the PP dataset as a “out-of-domain” dataset due to its substantial difference with regard to writing style and institution type compared to the CSU dataset²⁴.

Tagging performance

We present DeepTag’s performance on the CSU and PP test data in Table 1. To save space, we display the 21 most frequent disease codes in Table 1. Each SNOMED-CT code corresponds to one disease category. For each category, we report the number of training examples in the category (N), the scores for precision, recall, F_1 , accuracy, and the number of disease subtypes in this category. While DeepTag achieves reasonable F_1 scores overall, its performance is quite heterogeneous in different categories. Moreover the performance decreases when DeepTag is applied to the out-of-domain PP test data.

We identify two factors that substantially impact DeepTag’s performance: 1) the number of training examples that are tagged with the given disease label; 2) the number of subtypes, where a subtype is a SNOMED-CT code applied to either dataset that is lower in the SNOMED-CT hierarchy than the top-level disease category codes DeepTag is predicting.



(a)

CSU clinical note example

Jem is a 10 year old male castrated hound mix that was presented for continuation of chemotherapy for previously diagnosed B-cell multicentric lymphoma. Jem was started on CHOP chemotherapy last week and has been doing very well since receiving doxorubicin. The owners have noted his lymph nodes have gotten much smaller. He has some loose stool, yet improved with metronidazole. Current medications include prednisolone. Assessment: Jem is in a strong partial remission based on today's physical exam. He is also doing very well since starting chemotherapy. A CBC today was unremarkable and adequate for chemotherapy. She was dispensed oral cyclophosphamide and furosemide that the owners were instructed to give at home.

Expert annotated diseases: Disorder of hematopoietic cell proliferation, Neoplasm and/or hamartoma

PP clinical note example

Likely ear infection shaking head now swollen drooping ear otherwise doing well amulating well- had RF carpal arthrodesis at UCD. wt: 95.3 lbs. Ears/Eyes/Nose/Throat: Clear OU/ brown yeasty debris AU erythema AU no fb/tm;s intact AU mod aural hematoma AD Cardiovascular: No murmur/arrhythmia. Femoral pulses strong and synchronous. HR:84 Respiratory: Lungs sound clear bilaterally no crackles or wheezes. Eupneic. RR:20 Lymph nodes: No palpable peripheral lymphadenopathy Oral Exam: mm pink and moist. CRT < 2 sec Musculoskeletal: No lameness noted. Arthrodesis carpal joint RF thickened stifle LH ambulating well Nervous System: Appropriate mentation. No overt neurologic deficits Integument: Full haircoat. Adequate skin turgor. otitis externa AU aural hematoma AD. Ear cytology - ++cocci yeast AU. Cleaned with epiotic. Rx Tresaderm BID x 14 days. applied first dose Rx temarilP taper Skin prep medial AD over hematoma. then 19g butterfly needle attached to syringe drained 10ml bloody fluid held pressure with guaze no more bleeding CE: Recheck in 14d to ensure infection cleared discussed aural hematomas options for tx sx. may recur.

Expert annotated diseases: Infectious disease, Disorder of the integument, Disorder of the auditory system

(b)

Figure 1. System workflow and clinical note examples. Figure (a) shows the workflow of DeepTag with abstention. Then we show two example meta-categories corresponding to two subsets of the 42 SNOMED-CT codes. Figure (b) shows two example notes from the CSU and PP datasets. The highlighted text shows the supporting evidence human curators use to assign disease tags to these documents.

We use the number of subtypes as a proxy for the diversity and specificity of the clinical text descriptions. Thus, a higher number of subtypes is used

here as a proxy for a wider spectrum of diseases.

Table 1. Report of DeepTag performance on CSU test data and PP data

Disease	CSU						PP (Cross-hospital)					
	N	Prec	Rec	F_1	Accu	Sub	N	Prec	Rec	F_1	Accu	Sub
Autoimmune disease	1280	94.0	72.3	81.4	99.6	11	1	60.0	25.0	34.7	99.6	1(1)
Congenital disease	3345	72.9	35.9	47.3	97.8	224	17	58.0	5.3	9.2	97.1	8(6)
Propensity to adverse reactions	5105	89.1	70.2	78.1	98.2	8	43	83.6	13.2	21.3	93.0	7(2)
Metabolic disease	5265	68.9	55.4	61.0	96.9	82	26	75.8	51.1	59.8	96.5	12(9)
Disorder of auditory system	5393	81.0	66.2	72.8	97.7	67	64	76.8	69.4	72.4	95.0	12(6)
Hypersensitivity condition	6871	85.7	74.6	79.5	97.7	31	50	72.7	20.6	30.5	92.1	11(4)
Disorder of endocrine system	7009	79.2	66.7	72.2	96.9	84	46	71.5	28.2	40.1	92.6	8(8)
Disorder of hematopoietic cell proliferation	7294	95.1	87.4	91.0	98.9	22	16	68.6	31.0	41.1	97.5	6(1)
Disorder of nervous system	7488	76.1	63.8	69.2	96.4	243	27	68.0	31.7	41.6	94.9	19(14)
Disorder of cardiovascular system	8733	79.3	62.5	69.7	95.7	351	53	48.1	54.7	49.9	89.8	30(24)
Disorder of the genitourinary system	8892	77.7	62.6	69.3	95.7	317	44	59.9	40.3	47.2	92.3	19(12)
Traumatic AND/OR non-traumatic injury	9027	72.8	57.2	63.5	94.8	536	19	43.8	12.0	18.3	96.2	13(8)
Visual system disorder	10139	84.3	81.1	82.6	96.9	413	62	68.6	63.9	65.7	93.2	39(34)
Infectious disease	11304	71.2	53.7	60.8	92.9	260	88	56.3	21.9	30.2	86.7	20(10)
Disorder of respiratory system	11322	79.5	65.5	71.8	95.2	274	27	40.2	41.3	38.4	94.0	16(14)
Disorder of connective tissue	17477	75.4	67.0	70.7	91.3	567	24	38.4	31.2	33.8	94.3	15(11)
Disorder of musculoskeletal system	20060	77.0	73.4	74.8	91.1	670	56	66.4	45.4	53.2	91.5	31(19)
Disorder of integument	21052	84.2	71.6	77.3	92.3	360	156	55.7	58.5	56.8	80.6	58(32)
Disorder of digestive system	22589	76.8	67.1	71.5	89.7	694	195	54.7	48.4	50.2	72.7	47(36)
Neoplasm and/or hamartoma	36108	92.2	88.9	90.5	93.9	749	59	27.5	77.3	40.0	76.2	18(7)

This table reports the DeepTag’s performance (precision, recall, F_1 and accuracy) for the 21 most frequent disease categories (from a total of 42 categories). N indicates the total number of examples in the dataset. Sub indicates the number of specific disease codes that are present in the dataset that are binned into one of the disease level codes. For the PP dataset, the Sub number in parentheses indicate the number of subtypes that are also present in CSU dataset.

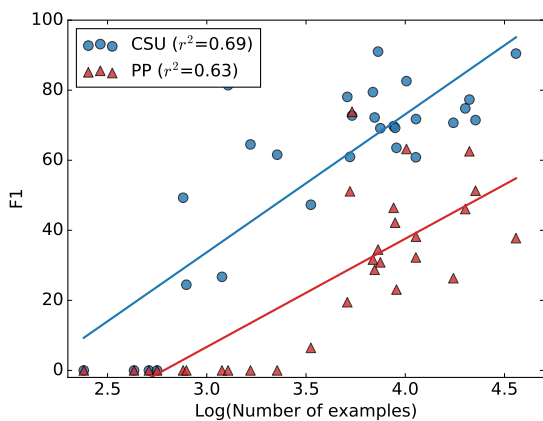


Figure 2. Per-label F_1 score plotted with log of number of examples in the training dataset.

Results shown here are from the DeepTag model. Each point represents a label, its corresponding number of training examples in CSU, and the per-label F_1 score from the DeepTag model.

Performance improves with more training examples. We first note that DeepTag works relatively well when the number of training examples for each label is abundant. We generate a scatter plot to capture the correlation between number of examples in the in CSU dataset and the label’s F_1 score evaluated

on the CSU test set. We also plot the F_1 score for the label evaluated on PP dataset and its number of training examples on CSU dataset.

For the CSU dataset, we observe an almost linear relationship between the log number of examples and the F_1 score in Figure 2. We observe a similar pattern when evaluating on PP dataset, though the correlation is weaker and the pattern is less linear. This is due to the out-of-domain nature of PP, which we investigate in depth below.

More diverse categories are harder to predict.

After observing the general correlation between number of training examples and per-label F_1 scores, we can investigate outliers. These are diseases that have many examples but on which the tagger performed poorly and diseases that have few examples but the tagger performed well. For *disorder of digestive system*, despite having the second highest number of training examples (22,589), both precision and recall are lower than other frequent diseases. We find that this disorder categories covers the second largest number of disease subtypes (694). On the other hand, *disorder of hematopoietic cell proliferation* has the highest F_1 score with relatively few training examples ($N = 7294$). This category has only 22 subtypes.

Table 2. Evaluation of trained classifiers on the CSU and PP data

Model	EM	Precision		Recall		F_1	
		unwgt	wgt	unwgt	wgt	unwgt	wgt
CSU data							
LSTM	47.4	76.6	85.9	59.3	78.7	65.3	81.7
BLSTM	48.2	76.1	86.0	57.6	79.4	63.5	82.2
DeepTag-M	48.6	76.8	86.3	58.7	79.6	64.6	82.4
DeepTag	48.4	79.9	86.1	62.1	79.8	68.0	82.4
PP data							
LSTM	13.8	48.1	65.7	31.8	51.9	33.8	54.4
BLSTM	13.8	47.3	66.0	35.6	57.9	36.9	58.4
DeepTag-M	17.1	53.4	68.0	37.9	59.9	40.6	61.1
DeepTag	17.4	56.5	70.3	41.4	62.4	43.2	63.4

Aggregate prediction performance across the 42 categories. BLSTM refers to the multi-task bidirectional LSTM. DeepTag is our best model, and DeepTag-M is the variation with a meta-category loss. EM indicates the exact match ratio, which is the percentage of the clinical notes where the algorithm perfectly predicts all of the disease categories. For example, if a note has three true disease labels, then the algorithm achieves an exact match if it predicts exactly these three labels, no more and no less. For each precision, recall and F_1 score, there are two ways to compute an algorithm’s performance. First we can take an unweighted average of the score across all the disease categories (unwgt) or we can take an average weighted by the number of test examples in each category (wgt).

Similarly *autoimmune diseases* has few training examples ($N = 1280$) but it still has a relatively high F_1 , and it also has only 11 subtypes.

The number of subtypes—i.e. the number of different types of lower level codes are mapped to each higher-level disease code—can serve as an indicator for the diversity or specificity of the text descriptions. For a disease like *disorder of digestive system*, it subsumes many different types of diseases such as *periodontal disease*, *hepatic disease*, and *disease of stomach*, which all have different diagnoses. Similarly, *Neoplasm and/or hamartoma* encapsulates many different histologic types and be categorized as benign, malignant, or unknown, thus resulting in many different lower-level codes (749 codes) being mapped into the same top-level disease code. The tagger needs to associate diverse descriptions to the same high-level label, increasing the difficulty of the tagging.

We hypothesize that disease labels with many subtypes will be difficult for the system to predict. This hypothesis suggests that the number of subtypes within a diagnosis category could explain some of the heterogeneity in DeepTag’s performance beyond the heterogeneity due to the training sample size. We conduct a multiple linear regression test with both the number of training examples as well as number of subtypes each label contains as covariates and the F_1 score as the outcome. In the regression, the coefficient for number of subtypes is negative with

$p < .001$. This indicates that, controlling for the number of training examples, having more subtypes in a disease category makes tagging more challenging and decreases DeepTag’s performance on the label.

Performance on PP Next we investigate DeepTag’s performance discrepancy between the CSU and PP test data. A primary contributing factor to the discrepancy is that the underlying text in PP is stylistically and functionally different from the text in CSU. Note that DeepTag was only trained on CSU text and was not fine-tuned on PP. The example texts in Figure 1b illustrate the striking difference. In particular, PP uses many more abbreviations that are not observed in CSU.

After filtering out numbers, 15.4% of words in PP are not found in CSU. Many of the PP specific words appear to be medical acronyms that are not used in CSU or terms that describe test results or medical procedures. Since these vocabulary has no trained and updated word embedding from the CSU dataset, the tagger will not be able to leverage them in the disease tagging process.

Despite having many training examples, DeepTag is doing poorly on some very frequent diseases, for example, *neoplasm and/or hamartoma*. On the opposite end of the spectrum, the tagger is able to do well for *disorder of auditory system* on both CSU and PP dataset, despite only having a moderate amount of training examples. Besides the main issue of vocab-

ulary mismatch, many subtypes (lower-level codes) that get mapped to a certain disease level code do not exist in PP, and subtypes in PP also might not exist in CSU. We refer to this as the subtype distribution shift.

For example, In CSU, *neoplasm and/or hamartoma* has 749 observed subtypes. Only 7 out of 749 subtypes are present in PP. Moreover there are 11 subtypes are unique to the PP dataset and are not observed in the CSU training set. These differences appear to be primarily due to differences in how the primary medical codes are applied to the datasets and not significant discrepancies in the types of neoplasias observed.

In addition to the subtype analysis, we note that for rarer diseases, the precision drop between CSU and PP is not as deep as the recall drop. This can be interpreted as the model is fairly confident and precise about the key phrases it discovered from the CSU dataset. However, the PP dataset uses other terms or phrases (that are not covered in the CSU dataset) to describe the disease, resulting in a sharper loss on recall.

Improvements from disease similarity

The 42 SNOMED-CT codes can be naturally grouped into 19 meta-categories; each meta-category corresponds to a subset of diseases that are related to each other^c. For example, the SNOMED-CT codes for “Disease caused by Arthropod” and “Disease caused by Annelida” belong to the same meta-category, “Infectious and parasitic diseases”. We designed DeepTag to leverage this hierarchical structure amongst the disease codes. Intuitively, suppose the true disease associated with a note is A and DeepTag mistakenly predicts code B . Then its penalty should be larger if B is very different from A —i.e., they are in different meta-categories—than if B and A are in the same meta-category. More precisely, we use the grouping of similar codes into meta-categories as a regularization in the training objective of DeepTag. Basic deep learning systems like LSTM and BLSTM do not incorporate this information.

DeepTag uses a L_2 -based distance objective to place this constraint between disease label embeddings. The objective encourages the embeddings of diseases that are in the same meta-category to be closer to each other than embeddings of diseases across meta-categories. In addition, we investigated

^cSee Supplementary Material for more information about the grouping.

another approach that can also leverage similarity: DeepTag-M. This method computes the probability of a parent-level code based on the probability of its children-level codes. Instead of forcing similarity/dissimilarity constraints on disease label embeddings, DeepTag-M encourages the model to make correct prediction on the parent level as well as on the child level.

In Table 2, we compare the performance of DeepTag, DeepTag-M, the standard multi-task LSTM and bidirectional LSTM (BLSTM). On the CSU dataset, DeepTag and DeepTag-M perform slightly better (or at the same capacity) compared to the baseline models (LSTM and BLSTM). DeepTag is able to have higher unweighted precision, recall, and F_1 score compared to the other models, indicating its ability to have good performance on a wide spectrum of diseases. The importance of leveraging similarity is shown on the PP dataset (Figure 3). Since it is out-of-domain, expert defined disease similarity provide much-needed regularization to make both DeepTag and DeepTag-M outperform baseline models by a substantial margin, with DeepTag being the overall best model.

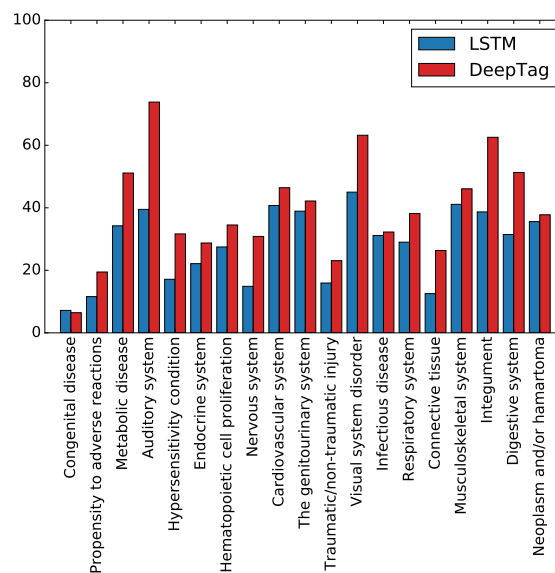


Figure 3. Performance comparison on PP. We compare the per-label F_1 score between baseline LSTM model and DeepTag model on the PP dataset. The disease categories are sorted from the least frequent to the most frequent in the training dataset, which comes from CSU.

Learning to abstain

Augmenting a tagging system with the ability to abstain (decline to assign codes) can foster human-

machine collaboration. When the system does not have enough confidence to make decisions, it has the option to defer to its human counterparts. This aspect is important in DeepTag because after tagging the documents, further analysis from various parties might be conducted on the tagged documents such as investigating the prevalence of certain specific diseases. In order to not mislead further clinical research, having the ability to abstain from making very erroneous predictions and ensuring highly precise tagging is an important feature.

We developed an additional abstention wrapper on top of DeepTag that we call DeepTag-abstain. The module learns to estimate how well the DeepTag system will perform on a document based on the predicted categories DeepTag makes on the document as well as DeepTag’s internal confidence on the predictions.

We compare DeepTag-abstain to an intuitive baseline where an abstention score is simply computed by the confidence associated with the diagnosis code assignments. In order to evaluate how well DeepTag-abstain performs compared to the baseline, we compute an abstention priority score for each document. A document with higher abstention priority score will be removed earlier than a document with low score. We then compute the weighted average of F_1 and exact match ratio (EM) for all the documents that are not removed.

For both baseline and DeepTag-abstain, we specify a proportion of the documents need to be removed. We adjust the dropped portion from 0 to 0.9 (dropping 90% of the examples at the high end). An abstention method that can drop more erroneously tagged documents earlier will observe a faster increase in its performance, corresponding to a curve with steeper slope.

DeepTag-abstain demonstrates a substantial improvement over the baseline in Figure 4. The baseline here is the natural approach that abstains based on the original DeepTag’s uncertainty at the last layer. DeepTag-abstain is a more powerful approach that *learns* where to abstain based on the model’s internal representation of the input text. We note that not all learning to abstain schemes are able to out-perform the baseline. The details of module design and improvement curve for the rest of the modules can be seen in Appendix Fig S2.

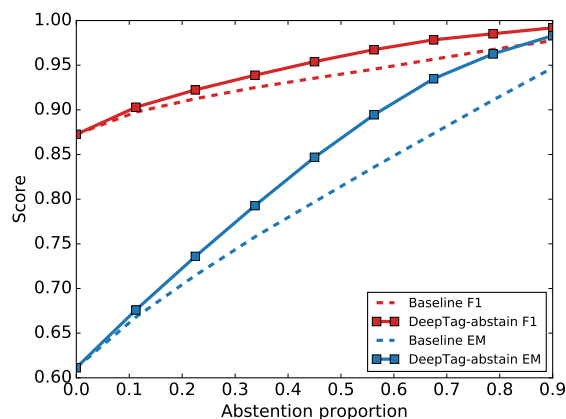


Figure 4. Comparison of the abstention models. DeepTag-abstain is the abstention priority score estimator that uses confidence scores as input and estimate instance-level accuracy of a given document. Baseline refers to the abstention scheme where the instance-level abstention priority score is computed from individual label confidence scores without any learning. As a greater proportion of the examples are abstained from, the performance— F_1 and Exact Match (EM)—of both methods improve. DeepTag-abstain shows faster improvement, indicating that it learns to abstain in more difficult cases.

Discussion

In this study, we developed a multi-label classification algorithm for veterinary clinical text, which represents a medical domain with an under-resourced medical coding infrastructure. In order to improve the performance of DeepTag on diseases with rare occurrences, we investigated with loss augmentation strategies that leverage the hierarchical structure of the disease categories. These augmentations provide gains over the LSTM and BLSTM baselines, which are common methods used for these types of prediction tasks. We also experimented with different methodologies to allow the model to learn to abstain on examples where the model is not confident in the predictions. We demonstrate that learned abstention rules outperform manually set rules.

Our work demonstrates novel methods for applying broad disease category labels to clinical records as well as applying those trained algorithms to an external dataset in order to examine cross-hospital generalization. We also demonstrate means to allow human domain experts to use their judgement where automated taggers have a high level of uncertainty in order to improve the overall workflow.

We confirm that cross-hospital generalization is a significant concern for learned tagging systems to be deployed in real world implementations that may vary substantially from the data on which they were trained. Even though our work attempts to mitigate this problem, there is significant research to be done in optimizing methods for domain adaptation. Our current work is important not only for veterinary medical records, which are rarely coded, but also may have implications for human medical records in countries with limited coding infrastructure and which are important regions of the world for public health surveillance and clinical research.

There are several aspects of the data that may have limited our ability to apply methods from our training set to our external validation set. Private veterinary practices often have data records that closely resemble the PP dataset used to evaluate our methods here. However, the large annotated dataset we used for training is from an academic institution (as these are, largely, the institutions that have dedicated medical coding staff). As can be seen from Table 2, the performance drop due to domain mismatch is non-negligible. The domain shift comes from two parts. First, text style mismatch – private commercial notes use more abbreviations and tend to include many procedural examinations (even though many are non-informative or non-diagnostic). This requires the model to learn beyond keyword or phrase matching. Second, label distribution mismatch – the CSU training dataset focuses largely on neoplasm and several other tumor-related diseases, largely due to the fact that the CSU hospital is a regional tertiary referral center for cancer and cancer represents nearly 30% of the caseload. Other practices will have datasets composed of labels that appear with different frequencies, depending on the specializations of that particular practice. A very important path forward is to use learning algorithms that are robust to domain shift, and experimenting with unsupervised representation learning to mitigate the domain shift between academic datasets and private practice datasets.

Currently we are predicting top-level SNOMED-CT disease codes, which are not the SNOMED-CT codes that have been directly annotated on the dataset. Many of the SNOMED-CT codes that are applied to clinical records are categorized as 'Findings' that are not actual 'Disorders' as the actual diagnosis of a patient may not be clear at the time the codes are applied. One example is an animal that is evaluated for 'vomiting' and the actual cause is not determined,

may have a code of 'vomiting(finding)'(300359004) applied and not 'vomiting(disorder)'(422400008) and these 'non-disorder' disease codes are not evaluated in our current work. However, these are an important subset of codes and represent another means to identify particular patient cohorts with particular clinical signs or presentations, vs. diagnosed disorders.

Another future direction for the abstention branch of this work is to factor human cost and annotation accuracy into the model and only defer when the model believes that human experts will bring improvement to the result within an acceptable amount of cost. This is an interesting direction for experimentation.

Methods

Datasets

Colorado State University dataset The CSU dataset contains discharge summaries as well as applied diagnostic codes for clinical patients from the Colorado State University College of Veterinary Medicine and Biomedical Sciences. This institution is a tertiary referral center with an active and nationally recognized cancer center. Because of this, the CSU dataset over-represents cancer-related diseases. Rare disease categories in the CSU dataset are diseases like pregnancy, perinatal and mental disorders, but these are also rare in the larger veterinary population as a whole and do not represent a dataset bias. Overall, there are 112,558 unique discharge summaries in CSU dataset. We split this dataset into training, validation, and test set by 0.9/0.05/0.05.

Private Practice dataset An external validation dataset was obtained from a regional private practice (PP). These records did not have diagnostic codes available and only approximately 3% of these records had free text diagnoses applied by the attending clinician. Two veterinary domain experts applied SNOMED-CT disease codes to a subset of these records and achieved consensus on the records used for validation. This dataset (PP) is used for external validation of algorithms developed using the CSU dataset. There are 586 documents in this external validation dataset.

Data processing

Documents in our corpus have been tagged with SNOMED-CT codes that describe the clinical conditions present at the time of the visit being annotated. Annotations are applied from the SNOMED-CT

veterinary extension (SNOMEDCT_VET), which is fully compatible and is an extension of the International SNOMED-CT edition. It can be accessed in a dedicated browser and is maintained by the Veterinary Terminology Services Laboratory at the Virginia-Maryland Regional College of Veterinary Medicine^d. Medical coders applying diagnostic codes are either veterinarians or trained medical coders with expertise in the veterinary domain and the SNOMED terminology. The medical coding staff at CSU utilize post-coordinated expressions, where required, for annotations to fully describe a diagnosed condition. For this work, we only considered the core disease codes and not the subsequent modifiers for training our models. The PP dataset was similarly coded using post-coordinated terms following consultation with coding staff at multiple academic institutions that annotate records using SNOMED-CT. We further grouped the 42 SNOMED-CT codes into 19 meta-categories. More details of this grouping are provided in the Supplement.

Difference in data structures

Due to the inherent differences in clinical notes/discharge summaries prepared for patients in an academic setting compared to the shorter 'SOAP' format notes (Subjective, Objective, Assessment, Plan) prepared in private practice, there are substantial differences in the format as well as the writing style and level of detail between these two datasets. In addition, the private practice records exhibit significant differences in record styles between clinicians, as some clinicians use standardized forms while others use abbreviated clinical notes containing only references to abnormal clinical findings.

As can be seen in Fig S1, both dataset have more than 80% documents associated with more than one label, and in terms of document length distribution, PP dataset document is much shorter than CSU dataset, while the average PP document length is 191 words. The average CSU document length is 325 words.

In order to bridge the gap between the two domains, we additionally use a curated veterinarian abbreviation list that maps an abbreviation to its full text. We include this abbreviation list in our supplementary materials.

^d<http://vts1.vetmed.vt.edu/default.cfm>

Algorithm development and analysis

We trained our modeling algorithm on CSU dataset and evaluated on a held-out portion of data from the CSU dataset as well as the PP dataset. We formulated our base model to be a recurrent neural network with long short-term memory cells (LSTMs). We additionally decided to run this recurrent neural network on both the forward direction and backward direction of the document (bidirectional), as is found beneficial in Graves et al.²⁵. We then built 42 independent binary classifiers to predict the existence of each label. This is the architecture found most useful in multi-label classification literature²¹. The model is trained jointly with binary cross entropy loss. We then augmented this baseline model with two losses: cluster penalty²⁶ and a novel meta-label prediction loss to leverage human expert knowledge in how semantically related these disease labels are.

We tuned the clustering penalty hyperparameters γ_{norm} , γ_{within} and γ_{between} , and our search range was [1e-1, 1e-5]. We also tuned the meta-label prediction loss hyperparameter β in a similar range.

Data availability

The data that support the findings of this study are available from Colorado State University College of Veterinary Medicine and a private practice veterinary hospital near San Francisco, but restrictions apply to the availability of these data, which were made available to Stanford for the current study, and so are not publicly available. Data are however available from the authors upon reasonable request and with permission of Colorado State University College of Veterinary Medicine and the private hospital.

Code availability

DeepTag is freely available at <https://github.com/windweller/DeepTag>.

Acknowledgements

We would like to acknowledge the help of Devin Johnsen for her help in annotating the private practice records used in this work. We also want to thank Selina Dwight and Matthew Wright for helpful feedback. Our work is funded by the Chan-Zuckerberg Investigator Program and National Science Foundation (NSF) Grant CRII 1657155.

Author contributions statement

A.N. performed the natural language processing work, designed and built DeepTag, and performed all of the experiments. A.Z. acquired the data, established the meta-hierarchies, organized and aided in annotation of the private practice data, and provided feedback on the NLP and machine learning outputs. R.P. provided access to the training data. A.P. aided in initial data acquisition and provided feedback on the project focus and strategy. M.R., S.D. and C.B. provided feedback on the project. J.Z. designed and supervised the project. A.N., A.Z. and J.Z. wrote the paper.

Additional information

Competing Interests: the authors declare no competing interests.

References

1. O'Neill, D. G., Church, D. B., McGreevy, P. D., Thomson, P. C. & Brodbelt, D. C. Approaches to canine health surveillance. *Canine genetics epidemiology* **1**, 2 (2014).
2. Kol, A. *et al.* Companion animals: Translational scientist's new best friends. *Sci. translational medicine* **7**, 308ps21–308ps21 (2015).
3. LeBlanc, A. K., Mazcko, C. N. & Khanna, C. Defining the value of a comparative approach to cancer drug development. *Clin. Cancer Res. clincanres*–2347 (2015).
4. Grimm, D. From bark to bedside (2016).
5. Klinck, M. P. *et al.* Translational pain assessment: could natural animal models be the missing link? *Pain* **158**, 1633–1646 (2017).
6. Baraban, S. C. & Löscher, W. What new modeling approaches will help us identify promising drug treatments? In *Issues in Clinical Epileptology: A View from the Bench*, 283–294 (Springer, 2014).
7. Hernandez, B. *et al.* Naturally occurring canine melanoma as a predictive comparative oncology model for human mucosal and other triple wild-type melanomas. *Int. journal molecular sciences* **19**, 394 (2018).
8. Jurafsky, D. & Martin, J. H. *Speech and language processing*, vol. 3 (Pearson London:, 2014).
9. Hochreiter, S. & Schmidhuber, J. Long short-term memory. *Neural computation* **9**, 1735–1780 (1997).
10. Goldberg, Y. Neural network methods for natural language processing. *Synth. Lect. on Hum. Lang. Technol.* **10**, 1–309 (2017).
11. Velupillai, S., Mowery, D., South, B. R., Kvist, M. & Dalianis, H. Recent advances in clinical natural language processing in support of semantic analysis. *Yearb. medical informatics* **10**, 183 (2015).
12. Demner-Fushman, D. & Elhadad, N. Aspiring to unintended consequences of natural language processing: a review of recent developments in clinical and consumer-generated text processing. *Yearb. medical informatics* 224 (2016).
13. Pivovarov, R. *et al.* Learning probabilistic phenotypes from heterogeneous ehr data. *J. biomedical informatics* **58**, 156–165 (2015).
14. Lipton, Z. C., Kale, D. C., Elkan, C. & Wetzel, R. Learning to diagnose with lstm recurrent neural networks. *arXiv preprint arXiv:1511.03677* (2015).
15. Pradhan, S. *et al.* Evaluating the state of the art in disorder recognition and normalization of the clinical narrative. *J. Am. Med. Informatics Assoc.* **22**, 143–154 (2014).
16. Jagannatha, A. N. & Yu, H. Bidirectional rnn for medical event detection in electronic health records. In *Proceedings of the conference. Association for Computational Linguistics. North American Chapter. Meeting*, vol. 2016, 473 (NIH Public Access, 2016).
17. Pradhan, S., Elhadad, N., Chapman, W., Manandhar, S. & Savova, G. Semeval-2014 task 7: Analysis of clinical text. In *Proceedings of the 8th International Workshop on Semantic Evaluation (SemEval 2014)*, 54–62 (2014).
18. Elhadad, N. *et al.* Semeval-2015 task 14: Analysis of clinical text. In *Proceedings of the 9th International Workshop on Semantic Evaluation (SemEval 2015)*, 303–310 (2015).
19. Baumel, T., Nassour-Kassis, J., Elhadad, M. & Elhadad, N. Multi-label classification of patient notes a case study on icd code assignment. *arXiv preprint arXiv:1709.09587* (2017).
20. Rajkomar, A. *et al.* Scalable and accurate deep learning with electronic health records. *npj Digit. Medicine* **1**, 18 (2018).

21. Kavuluru, R., Rios, A. & Lu, Y. An empirical evaluation of supervised learning approaches in assigning diagnosis codes to electronic medical records. *Artif. intelligence medicine* **65**, 155–166 (2015).
22. Subotin, M. & Davis, A. R. A method for modeling co-occurrence propensity of clinical codes with application to icd-10-pcs auto-coding. *J. Am. Med. Informatics Assoc.* **23**, 866–871 (2016).
23. Perotte, A. *et al.* Diagnosis code assignment: models and evaluation metrics. *J. Am. Med. Informatics Assoc.* **21**, 231–237 (2013).
24. Li, Q. Literature survey: domain adaptation algorithms for natural language processing. *Dep. Comput. Sci. The Graduate Center, The City Univ. New York* 8–10 (2012).
25. Graves, A., Fernández, S. & Schmidhuber, J. Bidirectional lstm networks for improved phoneme classification and recognition. In *International Conference on Artificial Neural Networks*, 799–804 (Springer, 2005).
26. Jacob, L., Vert, J.-p. & Bach, F. R. Clustered multi-task learning: A convex formulation. In *Advances in neural information processing systems*, 745–752 (2009).
27. Sorower, M. S. A literature survey on algorithms for multi-label learning. *Or. State Univ. Corvallis* **18** (2010).
28. Mikolov, T. Statistical language models based on neural networks. *Present. at Google, Mountain View, 2nd April* (2012).
29. Collobert, R. & Weston, J. A unified architecture for natural language processing: Deep neural networks with multitask learning. In *Proceedings of the 25th international conference on Machine learning*, 160–167 (ACM, 2008).
30. Cortes, C., DeSalvo, G. & Mohri, M. Learning with rejection. In *International Conference on Algorithmic Learning Theory*, 67–82 (Springer, 2016).
31. Niculescu-Mizil, A. & Caruana, R. Predicting good probabilities with supervised learning. In *Proceedings of the 22nd international conference on Machine learning*, 625–632 (ACM, 2005).
32. Pennington, J., Socher, R. & Manning, C. Glove: Global vectors for word representation. In *Proceedings of the 2014 conference on empirical methods in natural language processing (EMNLP)*, 1532–1543 (2014).
33. Kingma, D. P. & Ba, J. Adam: A method for stochastic optimization. *arXiv preprint arXiv:1412.6980* (2014).
34. Klambauer, G., Unterthiner, T., Mayr, A. & Hochreiter, S. Self-normalizing neural networks. In *Advances in Neural Information Processing Systems*, 972–981 (2017).

Supplementary Materials

CSU discharge summary format

The Colorado State University discharge summaries contain multiple data fields, including: History, Assessment, Diagnosis, Prognosis, FollowUpPlan, ProceduresAndTreatments, PendingDiagnostics, PendingDiagnosticsComments, Diet, Exercise, DischargeStatus, DischargeDate, Medications, AdditionalInstructions DrugWithdrawal, RecheckVisits, Complications, MedicalComplications, SurgicalComplications and AnesthesiaComplications. We filtered out fields with many null entries as well as the diagnosis related fields, since this is not present in the private practice data. The remaining fields—History, Assessment, Prognosis, DischargeStatus and Medications—were used as the input to train the models.

Model description

We formulate the problem of veterinary disease tagging as a multi-label classification problem. Given a veterinary record X , which contains detailed description of the diagnosis, we try to infer a subset of diseases $\mathbf{y} \in \mathbf{Y}$, given a pre-defined set of diseases \mathbf{Y} . The problem of inferring a subset of labels can be viewed as a series of independent binary prediction problems²⁷. The binary classifier learns to predict whether a tag y_i exists or not for $i = 1, \dots, m$, where $m = |\mathbf{Y}|$.

Our learning system has two components: a text processing module and tag prediction module. Our text processing module will use long-short-term memory networks (LSTMs) which have demonstrated their effectiveness in learning implicit language patterns from the text²⁸. Our tag prediction module will consist of binary classifiers that are parameterized independently.

A long-short-term memory networks is a recurrent neural network with LSTM cell. It takes one word as input, as well as the previous cell and hidden state. Given a sequence of word embeddings x_1, \dots, x_T , the recurrent computation of LSTM networks at a time step t can be described in Eq 1, where σ is the sigmoid function $\sigma = 1/(1 + e^{-x})$, and \tanh is the hyperbolic tangent function. We use \odot to indi-

cate the hadamard product.

$$\begin{aligned} f_t &= \sigma(W_f x_t + V_f h_{t-1} + b_f) \\ i_t &= \sigma(W_i x_t + V_i h_{t-1} + b_i) \\ o_t &= \sigma(W_o x_t + V_o h_{t-1} + b_o) \\ \tilde{c}_t &= \tanh(W_c x_t + V_c h_{t-1} + b_c) \\ c_t &= f_t \odot c_{t-1} + i_t \odot \tilde{c}_t \\ h_t &= o_t \odot \tanh(c_t) \end{aligned} \quad (1)$$

An extension of this recurrent neural network with LSTM cell is to introduce bidirectional passes²⁵. Graves et al. shows that introducing bidirectional passes, it can effectively eliminate problems such as retaining long-term dependency when the document is very long. We parameterize two LSTM cells with different set of parameters, one cell is used in forward pass where the sequence is passed in sequentially from the beginning $\{x_1, \dots, x_T\}$, one cell is used for backward pass, where the sequence is passed in with reversed ordering $\{x_T, \dots, x_1\}$. At the end of both passes, bidirectional LSTM will output two hidden states represents each input x_t , and we stack these two hidden states as our new hidden state for this input $h_t = [\overrightarrow{h}_t; \overleftarrow{h}_t]$.

After computing hidden states over the entire documents, we introduce global max pooling over the hidden states, as suggested by Collobert & Weston²⁹ so that the hidden states will aggregate information from the entire documents. Assuming the dimension of hidden state is d , global max pooling apply an element-wise maximum operation over the temporal dimension of the hidden state matrix, described in Eq 2.

$$\begin{aligned} H &= [h_1, \dots, h_T], H \in \mathbb{R}^{T \times d} \\ c_j &= \max(H_j), \text{ for } j = 1, \dots, d \end{aligned} \quad (2)$$

Then we define a binary classifier for each label in our pre-defined set. The binary classifier takes in a vector \mathbf{c} that represents the veterinary record and outputs a sufficient statistic for the Bernoulli probability distribution indicating the probability of whether a tag should be predicted. For $i = 1, \dots, m$:

$$p(y_i) = \hat{y}_i = \sigma(\theta_i^T \mathbf{c}) \quad (3)$$

We use binary cross entropy loss averaged across all labels as the training loss. Given the binary predictions from the model $\hat{\mathbf{y}} \in [0, 1]^m$ and correct one-hot

label $\mathbf{y} \in \{0, 1\}^m$, binary cross entropy loss is written as follow:

$$\mathcal{L}_{\text{BCE}}(\hat{\mathbf{y}}, \mathbf{y}) = -\frac{1}{m} \sum_{i=1}^m y_i \log(\hat{y}_i) + (1 - y_i) \log(1 - \hat{y}_i) \quad (4)$$

As usual, the decision boundary in our model is 0.5. We can generate a list of predicted label by applying a decision function d :

$$d(\hat{y}_i) = \begin{cases} 0 & \text{if } \hat{y}_i \leq 0.5 \\ 1 & \text{if } \hat{y}_i > 0.5 \end{cases} \quad (5)$$

Leveraging disease similarity

We introduce two penalties that are inspired by the implicit relationships between the SNOMED-CT disease codes that we refer to as meta-labels or clusters. By augmenting our loss with these two penalties, we aim to increase model’s ability to predict labels that have fewer instances. In the result section, we refer to model trained with cluster penalty as “DeepTag”, and model trained with meta-label prediction loss as “DeepTag-M”.

Cluster penalty After defining the meta-labels for the SNOMED-CT disease tags, we can use techniques from multi-task learning literature. Jacob et al.²⁶ proposed a hypothesis that if two tasks are similar, the task-specific parameters for these two tasks should be close in vector space, vice versa.

Following Jacob et. al, we can first compute the mean vector of all tasks $\bar{\theta} = \frac{1}{m} \sum_{i=1}^m \theta_i$. We can define $\mathcal{J}(k) \subset \{1, \dots, m\}$, where $\mathcal{J}(k)$ is a set of labels that belong to cluster k . Then we can compute the mean vector for each cluster of tasks: for $k = 1, \dots, K$, $\bar{\theta}_k = \frac{1}{|\mathcal{J}(k)|} \sum_{i=1}^{|\mathcal{J}(k)|} \theta_i$.

The within-cluster closeness constraint Ω_{within} can be computed as the distance between task specific weight vectors and the cluster mean vector $\bar{\theta}_k$. Ω_{between} can be computed as the distance between $\bar{\theta}_k$ and $\bar{\theta}$. We formulate this as an additional loss term $\Omega(\Theta)$, and allow three hyperparameter γ_{norm} , γ_{within}

and γ_{between} to control the strength of this penalty.

$$\begin{aligned} \Omega_{\text{norm}} &= \sum_{i=1}^m \|\theta_i\|^2 \\ \Omega_{\text{between}} &= \sum_{k=1}^K \|\bar{\theta}_k - \bar{\theta}\|^2 \\ \Omega_{\text{within}} &= \sum_{k=1}^K \sum_{i \in \mathcal{J}(k)} \|\theta_i - \bar{\theta}_k\|^2 \end{aligned} \quad (6)$$

Meta-label prediction loss We propose an additional penalty following the intuition that we want the model to make accurate predictions for the broad category even though mistakes can be made on the fine-grained level. Meta labels are created by examining whether any disease label under this meta label has been marked as tagged. Following the same logic, since the disease labels are predicted independently, we can compute the probability of the presence of a meta label \tilde{y}_k from the probability of disease labels that belong to this meta label.

$$\begin{aligned} p(\tilde{y}_k) &= 1 - \prod_{i \in \mathcal{J}(k)} (1 - p(y_i)) \\ &= 1 - \prod_{i \in \mathcal{J}(k)} (1 - \sigma(\theta_i^T \mathbf{c})) \end{aligned} \quad (7)$$

After computing the probability of presence of each meta-label, given the set of meta labels $\tilde{\mathbf{y}}$ that are created from our true set of labels \mathbf{y} , we can then compute the binary cross entropy loss between the model’s estimation on meta label probability and true meta labels in Eq 8. We use β to adjust the strength of this penalty.

$$\begin{aligned} \mathcal{L}_{\text{meta}}(p(\tilde{\mathbf{y}}), \tilde{\mathbf{y}}) &= -\frac{1}{K} \sum_{k=1}^K \tilde{y}_k \log(p(\tilde{y}_k)) \\ &\quad + (1 - \tilde{y}_k) \log(1 - p(\tilde{y}_k)) \end{aligned} \quad (8)$$

Learning to abstain

In practice, it is often desirable for the model to forfeit the prediction if the prediction is likely to be incorrect. When the method is used in collaboration with human experts, the model can just defer difficult cases to them, fostering human-computer collaboration. However, this is still an under-explored field in machine learning, and previous research has focused largely on binary-class single-label classification³⁰. We formally describe the set-up and our learning-based approach in the following sections, and extend relevant discussion to a multi-label setting.

We propose two abstention settings. Each setting will compute a score α for each document, which we refer to as the abstention priority score. We can then rank these documents using this score α . When user specifies a percentage of documents to be dropped, documents that have high α will be dropped first.

Confidence-based abstention Since our model already outputs a probability for each label, if our model is well-calibrated, meaning that the output probability satisfies the following constraint in Eq 9, then our probability should reflect how uncertain the model is about the output.

$$P_{x,y \sim \mathcal{D}}[y = 1 | f_i(x) = p] = p \quad \forall p \in [0, 1] \text{ and } \forall t \quad (9)$$

The notion of calibration means that when the model thinks the chance of a given prediction to be correct is $p\%$, we collect all instances that the model gives such probability, and the model in total will be correct $p\%$ of the time. A well-calibrated model’s output probability corresponds to the model’s confidence/certainty on how correct its prediction is. Previous research has shown that binary classifiers with sigmoid scoring function and cross-entropy loss are often well-calibrated³¹.

Given calibrated $\{p(y_1), \dots, p(y_m)\}$, we want to compute how confident the model is on these predictions. Noticeably, For each prediction, the model is more confident if $p(y_i)$ is farther away from 0.5. Based on this observation, we can convert the probability into a confidence score with function g :

$$g(p(y_i)) = \begin{cases} 1 - p(y_i) & \text{if } p(y_i) \leq 0.5 \\ p(y_i) & \text{if } p(y_i) > 0.5 \end{cases} \quad (10)$$

We can now compute the probability of the model getting k labels correct on a single example. We choose all subsets from the entire label set, and compute the probability of a chosen subset to be correct as well as the probability of the not chosen ($m - k$) labels to be incorrect.

$$\alpha_{\text{conf}} = \sum_{\substack{I \subset \{1, \dots, m\} \\ |I|=k}} \left(\prod_{i \in I} g(p(y_i)) \right) \left(\prod_{j \notin I} 1 - g(p(y_j)) \right) \quad (11)$$

The score α_{conf} is an abstention priority score because it is a valid indication of how confident the model’s overall output is. We refer to this scheme confidence-based abstention module (or “CB” in Figure S2, “Baseline” in Figure 4).

Learning-based abstention Instead of computing α from a fixed formula, we can try to link abstention priority score to a value that we care about. For example, we want to drop examples that will induce high loss, or equivalently, examples where predicted result gives a low accuracy. However, we do not have access to ground-truth answers in the real world, instead, we propose that if the data distribution \mathcal{D} between training and deployment are consistent ($x_{\text{test}}, y_{\text{test}} \sim \mathcal{D}$, which is the underlying assumption specified in calibration), then we can learn to estimate loss or accuracy for each example. We can compute a regression target for the learned abstention module using the training dataset’s accuracy and loss value for each example (Eq 12).

$$\begin{aligned} \alpha_{\text{accu}}^i &= \frac{1}{m} \sum_{j=1}^m I(d(\hat{\mathbf{y}})_j, \mathbf{y}_j^i) \\ \alpha_{\text{loss}}^i &= \mathcal{L}_{\text{BCE}}(\hat{\mathbf{y}}^i, \mathbf{y}^i) \end{aligned} \quad (12)$$

This abstention learning module A can take an input z and output an estimated abstention score $\hat{\alpha}$. We train this module by minimizing minimum square squared error with the regression target:

$$\begin{aligned} \hat{\alpha}^i &= A(z^i) \\ \mathcal{L}_{\text{MSE}} &= \sum_{i=1}^N (\alpha^i - \hat{\alpha}^i)^2 \end{aligned} \quad (13)$$

We choose four possible inputs from various parts of the DeepTag model that the DeepTag-abstention module can use to predict accuracy or loss without knowing the ground-truth label. Two choices are obvious: confidence scores $g(\hat{\mathbf{y}})$ that is used to compute confidence-based abstention priority score in the previous section, and estimated probability for the presence of each label $\hat{\mathbf{y}}$, which we have used to compute confidence scores via function $g(\cdot)$. However, since $\hat{\mathbf{y}}$ is obtained by applying a sigmoid function to the output of the classifier $\hat{\mathbf{y}}_i = \sigma(\theta_i^T \mathbf{c})$, then we can also use the prior-to-sigmoid value $\theta_i^T \mathbf{c}$ as input. At last, we hypothesize that the representation of document \mathbf{c} might also contain relevant information that is useful for model A to determine whether the document is difficult to process.

We fit the model A to estimate α_{learn} in the training set of our data, same split as the one used to train the overall model. We then evaluate on a previously unseen test set.

Experimental Details

We initialize our model with 100-dimension GloVE word vectors³², and we initialize un-matched words in the CSU training data with sampled multivariate normally distributed vectors. We allow all word embeddings to be updated through the training process. We use a recurrent neural network with a 512 dimension LSTM cell, and set the feed-forward dropout rate to be 20%. We use batch size of 32, clipping gradient at 5. We use ADAM³³ optimizer with a learning rate of 0.001.

We trained all models to the maximum of 5 epochs with early stopping, the maximum number of epoch is picked by observing performance on validation dataset. After picking out the best hyperparameters on validation set, we evaluate all models in-domain generalization performance on the CSU test dataset and out-domain generalization performance on the PP dataset.

After hyperparameter searching, we report models with the hyperparameters that perform well on each dataset. We train each model five times and report the averaged result. For the CSU dataset, we find $\beta = 0.001$ works best for DeepTag-M, and $\gamma_{\text{norm}} = 1e-5$, $\gamma_{\text{between}} = 1e-4$, $\gamma_{\text{within}} = 1e-4$ works best for DeepTag (cluster penalty). For the PP dataset, we find $\beta = 0.0001$ works the best for DeepTag-M, and $\gamma_{\text{norm}} = 1e-4$, $\gamma_{\text{between}} = 1e-3$, $\gamma_{\text{within}} = 1e-3$ works best for DeepTag (cluster penalty). We report these results in Table 2.

For Table 1, we report DeepTag trained with $\gamma_{\text{norm}} = 1e-4$, $\gamma_{\text{between}} = 1e-3$, $\gamma_{\text{within}} = 1e-3$ and we regard this as our best setting.

Abstention Experimental Details

We use a 3-layer neural network with SELU activation³⁴ to parameterize abstention model A. The learning to abstain model is trained on various outputs generated by the DeepTag system after training the bidirectional LSTM with cluster penalty. All configurations of learning to abstain models are trained optimally for 3 epochs on the training set, and evaluated on the unseen test set.

SNOMED Meta-categories

Here we provide the full list of the SNOMED-CT meta-categories that we used to regularize the training objective of DeepTag. In the list, the numbers correspond to the meta-categories, and the letters indicate the original SNOMED-CT codes. We manually clustered the 42 SNOMED-CT codes into these

19 meta-categories, using the analogous clustering of the ICD-9 categories as a guide.

1. Complications of pregnancy, childbirth, and the puerperium
 - (a) Disorder of labor / delivery (disorder)
 - (b) Disorder of pregnancy (disorder)
 - (c) Disorder of puerperium (disorder)
2. Diseases of the genitourinary system
 - (a) Disorder of the genitourinary system (disorder)
3. Diseases of the musculoskeletal system and connective tissue
 - (a) Disorder of connective tissue (disorder)
 - (b) Disorder of musculoskeletal system (disorder)
4. Diseases of the skin and subcutaneous tissue
 - (a) Angioedema and/or urticaria (disorder)
 - (b) Disorder of pigmentation (disorder)
 - (c) Disorder of integument (disorder)
5. Certain conditions originating in the perinatal period
 - (a) Disorder of fetus or newborn (disorder)
6. Congenital anomalies
 - (a) Hereditary disease (disorder)
 - (b) Congenital disease (disorder)
 - (c) Familial disease (disorder)
7. Injury and poisoning
 - (a) Disorder caused by exposure to ionizing radiation (disorder)
 - (b) Poisoning (disorder)
 - (c) Traumatic AND/OR non-traumatic injury (disorder)
 - (d) Self-induced disease (disorder)
8. Symptoms, signs, and ill-defined conditions
 - (a) Hyperproteinemia (disorder)
 - (b) Clinical finding (finding)
9. Neoplasms

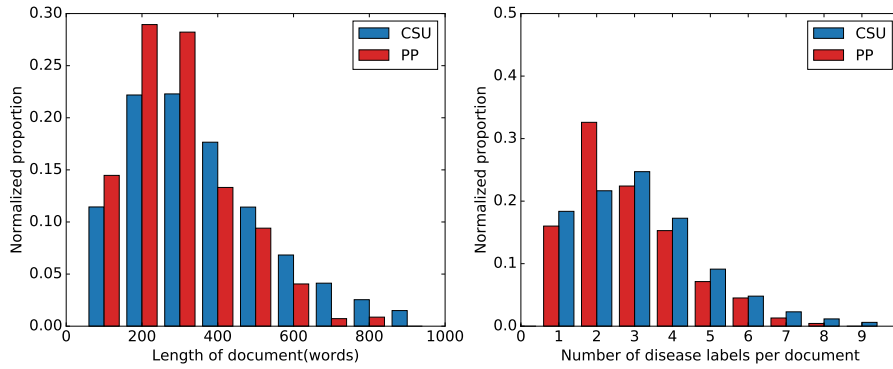


Figure S1. Document length and label distribution on CSU and PP dataset. Proportion of records in each dataset with certain length (number of words) or certain number of labels.

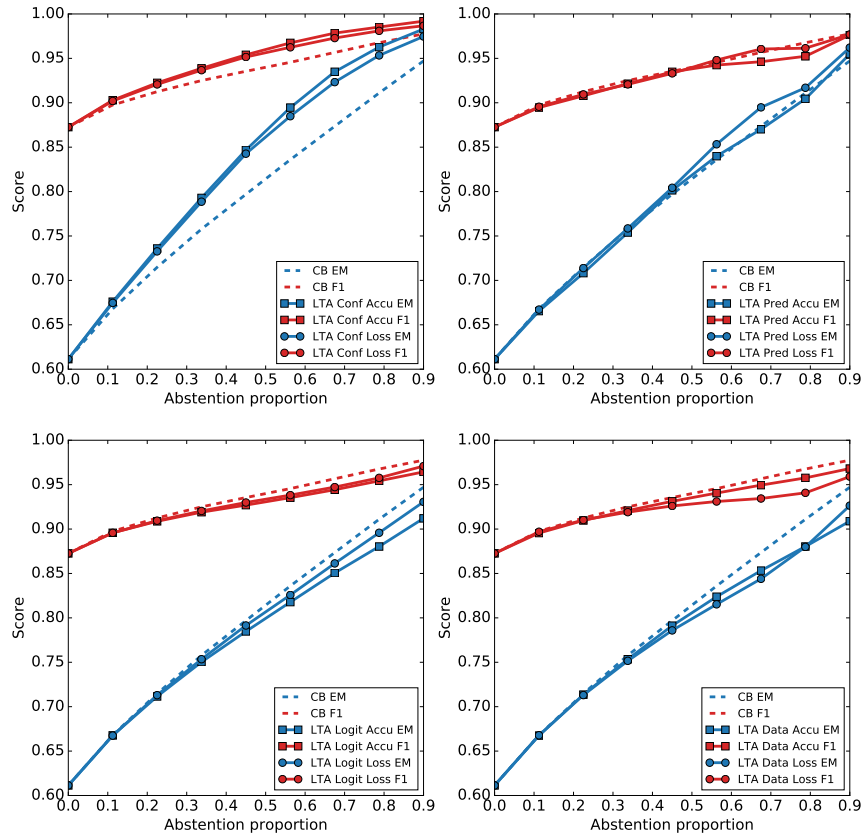


Figure S2. Abstention improvement curve. Top-left: learning to reject model with confidence score as input, estimate accuracy or loss. Top-right: learning to reject model with post-sigmoid probabilities \hat{y} score as input, estimate accuracy or loss. Bottom-left: learning to reject model with prior-to-sigmoid logits as input, estimate accuracy or loss. Bottom-right: learning to reject model with global max pooled hidden states \mathbf{c} as input, estimate accuracy or loss.

- (a) Neoplasm and/or hamartoma (disorder)
- (b) Fibromatosis (disorder)
- 10. Infectious and parasitic diseases
 - (a) Disease caused by Arthropod (disorder)
 - (b) Disease caused by Annelida (disorder)
 - (c) Infectious disease (disorder)
 - (d) Disease of presumed infectious origin (disorder)
 - (e) Disease caused by parasite (disorder)
 - (f) Enzootic disease (disorder)
 - (g) Epizootic disease (disorder)

11. Diseases of blood and blood-forming organs
 - (a) Anemia (disorder)
 - (b) Disorder of cellular component of blood (disorder)
 - (c) Disorder of hematopoietic cell proliferation (disorder)
 - (d) Disorder of hemostatic system (disorder)
 - (e) Spontaneous hemorrhage (disorder)
 - (f) Hyperviscosity syndrome (disorder)
 - (g) Secondary and recurrent hemorrhage (disorder)
 - (h) Secondary hemorrhage (disorder)
12. Endocrine, nutritional and metabolic diseases, and immunity disorders
 - (a) Autoimmune disease (disorder)
 - (b) Disorder of immune function (disorder)
 - (c) Hypersensitivity condition (disorder)
 - (d) Metabolic disease (disorder)
 - (e) Nutritional deficiency associated condition (disorder)
 - (f) Nutritional disorder (disorder)
 - (g) Obesity (disorder)
 - (h) Obesity associated disorder (disorder)
 - (i) Propensity to adverse reactions (disorder)
 - (j) Disorder of endocrine system (disorder)
13. Diseases of the nervous system
14. Feline hyperesthesia syndrome (disorder)
 - (a) Disorder of nervous system (disorder)
15. Mental disorders
 - (a) Mental disorder (disorder)
16. Diseases of the circulatory system
 - (a) Disorder of cardiovascular system (disorder)
17. Diseases of sense organs
 - (a) Disorder of auditory system (disorder)
 - (b) Vertiginous syndrome (disorder)
 - (c) Visual system disorder (disorder)
 - (d) Sensory disorder (disorder)
18. Diseases of the digestive system
 - (a) Vomiting (disorder)
 - (b) Enterotoxemia (disorder)
 - (c) Disorder of digestive system (disorder)
19. Diseases of the respiratory system
 - (a) Disorder of respiratory system (disorder)